How Accurately Can We Predict Optical Clarity in the Littorals?

Jeffrey H. Smart

The optical clarity of littoral waters directly impacts the performance of optics-based Navy systems being developed for mine and anti-submarine warfare. In particular, the optical detection and identification of near-surface mines and submarines depends on near-surface optical properties, but surface properties can be very different from bottom optical properties, which are relevant to optical identification of bottom mines. Using data collected recently in the Yellow Sea, Persian Gulf, and East China Sea, this article describes what we have learned about persistent features of near-surface and near-seafloor optical conditions. It will be shown that some localities (such as the central Yellow Sea) have relatively clear surface waters, while bottom conditions can be an order of magnitude more turbid. These results directly affect the utility of certain mine countermeasures and anti-submarine warfare systems.

INTRODUCTION

Optical clarity is a concept with which virtually everyone has some practical experience. For example, a river changes from crystal clear one day to brown and opaque the next (usually due to a major rainstorm that washes in sediments), or near-shore ocean waters change from clear on a calm day to murky the next (when large breaking waves are stirring up the bottom sediments). Water clarity (and color) also changes as a function of the concentration and species of suspended biologics, and effluents from rivers and estuaries carrying colored, dissolved organic materials impact water clarity in near-shore ocean regions.

The oceanographic community has been studying these phenomena for many years. An initial attempt at classifying "types" of water color/clarity was developed by Jerlov in the 1950s.[1] Jerlov produced generic curves for the attenuation of diffuse light as a function of wavelength. His clearest ocean waters were categorized as Type I, intermediate waters as Type II, and the murkiest waters as Type III; more turbid coastal waters were given values of 1 to 9 (9 being the least clear).[2] The near-surface data to be presented in this article generally span the Jerlov oceanic realm of Type I to Type III.

Optical clarity (or lack thereof) can significantly impact the utility of several Navy systems being developed for mine warfare (MIW) and anti-submarine warfare (ASW). A previous *Technical Digest* article described optical variability in the open ocean.[3] The present article presents several examples of the high degree of spatial variability in optical clarity as a function of location and depth domain in littoral areas of the western Pacific Ocean and Middle East. Particular attention is paid to

GLOSSARY

Δz: In oceanography, denotes thickness; z denotes depth.

Backscattering coefficient (b_b): Rate of decrease in backscattered light.

Beam attenuation coefficient (c): Rate of decrease in a collimated light source due to the combined effects of scattering and absorption.

Diffuse attenuation coefficient (K or K_d): Rate of decrease in a diffuse light source due to the combined effects of backscattering and absorption.

Inherent optical properties (IOPs): Parameters unaffected by viewing conditions (beam attenuation, absorption, scattering, etc.).

Mesoscale variability: Horizontal variability on scales of tens to hundreds of kilometers; usually refers to fronts and eddies.

Nepheloid layer: Water near the seafloor that contains high concentrations of suspended sediments.

the effect of the nepheloid layer on optical attenuation and optical scattering. Specific questions we will address include the following:

- How much does the nepheloid layer vary in intensity and vertical extent?
- How clear are the "surface" waters?
- How does optical clarity vary in time?
- How do strong tidal currents affect clarity?

Nepheloid layer optics are important because several MIW systems use optical sensors to identify bottom objects, in particular the AN/AQS-24 and AN/AQS20 mine-hunting/detection systems. On the other hand, the optical detection and identification of near-surface mines and submarines depend on near-surface optical properties. Several MIW and ASW systems (especially those for detection of near-surface objects) are either operational or in development. Active (laser-based) systems include the ALMDS (Airborne Laser Mine Detection System), AMNS (Airborne Mine Neutralization System), RAMICS (Rapid Airborne Mine Clearance System), and AN/AQS-20X (Advanced Airborne Mine Sensor). Passive (hyperspectral) systems include COBRA (Coastal Battlefield Reconnaissance and Analysis) and the LASH-ASW (Littoral Airborne Sensor-Hyperspectral Anti-Submarine Warfare) System. (The latter passively exploits the visible and near-infrared spectrum using hyperspectral processing with spatial filtering. See Ref. 4.) Besides these "high tech" systems, explosive ordnance disposal divers and remotely operated vehicles used for mine neutralization also depend on optical clarity.

To this point the optical state of the water has been described using the layman's term "clarity." A more proper discussion requires more scientifically accurate nomenclature, and the specific optical parameter that most affects a system's performance varies depending on the sensor technology. For example, for systems that use a wide field-of-view receiver with a lidar sensor, the environmental factors that impact performance are the diffuse attenuation coefficient (K) and optical backscattering (b_b) at 180°. The latter is very difficult to measure, but is highly correlated with optical backscattering between 90° and 180°. For systems that employ a laser-line scanner, performance depends on the beam attenuation coefficient (c). In addition, optical penetration is a function of wavelength.

The active optical systems described in this article use lasers at 532 nm, so most of the data displays are provided at that wavelength. Readers should, however, keep in mind that passive systems (including the human eye) generally "see" across a band of wavelengths, and the beam and diffuse attenuation coefficients can vary greatly across these bands. (For instance, in clear, open ocean waters, K at 490 nm may be 0.03/m compared to 0.06/m at 532 nm, i.e., there can be a factor of 2 change between the blue and green part of the visible spectrum.)

PERFORMANCE DATA

Western Pacific Ocean Littoral

Remote-sensing estimates of optical properties obtained from satellites are routinely used to estimate the spatial variability of optical conditions for several reasons. First, satellites provide data in denied areas (such as within the territorial waters of potentially hostile nations). Second, they provide a near-synoptic view in one or two passes, whereas comparable area coverage from *in situ* measurements would take days to months to obtain. Third, they are far less costly to use than manned systems.

An example of satellite-derived optical variability data for the Western Pacific Ocean is shown in Fig. 1. The data used are NASA's Coastal Zone Color Scanner (CZCS) 7-year seasonal average near-surface chlorophyll pigment concentrations. K at 532 nm can be computed from the pigment concentration using Morel's empirical equations[5] (note the K scale appended to the right of the pigment scale in Fig. 1; both are nonlinear). Although these 3-month seasonal averages tend to wash out mesoscale variability, they still capture some major features. For example, the deep open ocean areas east of Taiwan and south of Japan tend to be almost devoid of chlorophyll, implying that they have very low K values. Purple and dark blue regions are very clear (near the pure-water K532-nm value of 0.054/m); in contrast, the littoral areas of the Sea of Japan, and especially the shallow Yellow Sea, exhibit substantially higher pigment and K values, and there is more seasonal variability. The region east of the Yangtze River is especially interesting in that there appears to be a large "plume" of

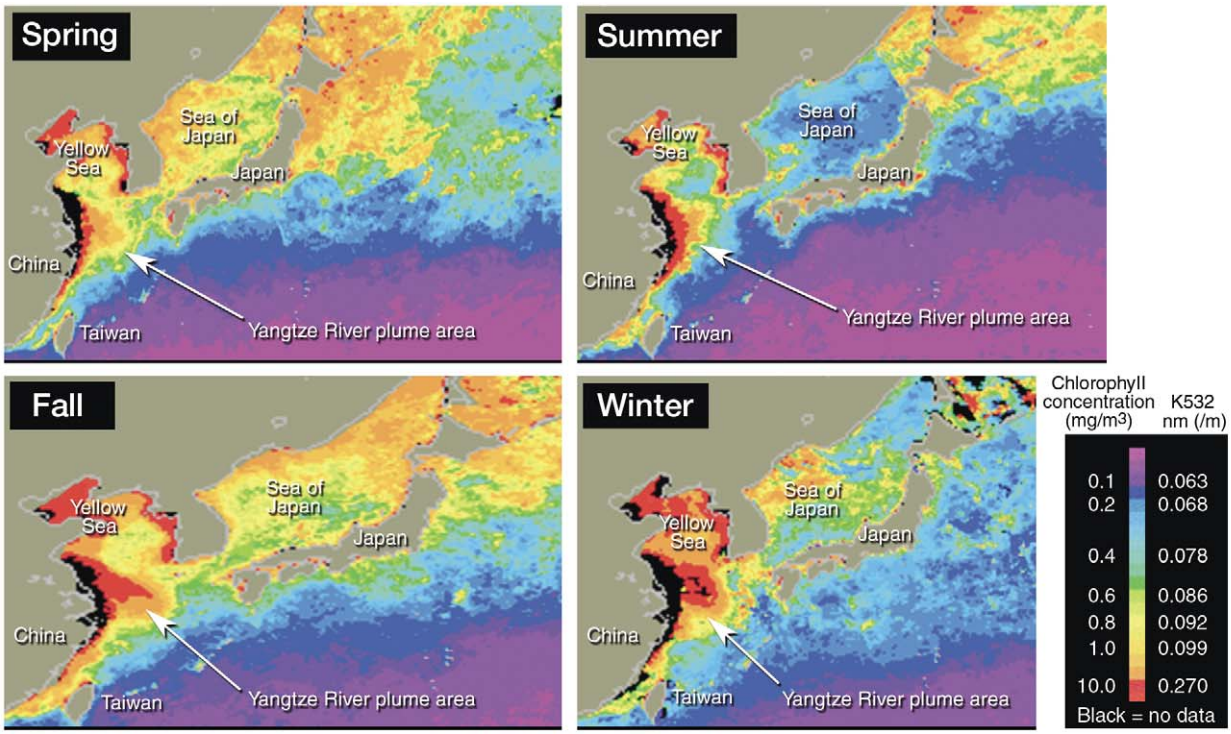

Figure 1. Example of spatial variability as seen from space: NASA CZCS 7-year composite surface chlorophyll images. The deep open ocean areas east of Taiwan and south of Japan (purple and dark blue, respectively) tend to be almost devoid of chlorophyll, i.e., they have very low K values. In contrast, the littoral areas of the Sea of Japan, and especially the shallow Yellow Sea, exhibit substantially higher pigment and K values as well as more seasonal variability. The region east of the Yangtze River is particularly interesting as there appears to be a large "plume" of more attenuating water with varying intensity and extent that is associated with the outflow of this major Chinese river.

more attenuating water with varying intensity and extent that is associated with the outflow of this major Chinese river.

Despite the relatively high concentrations of absorbing/attenuating pigments in the Yellow Sea surface waters, there is a central region that has relatively clear waters for all but the winter months. An examination of the bathymetry for the area (Fig. 2) shows that the central Yellow Sea is markedly deeper than the areas nearer the coast. In addition, the Yangtze River plume area is significantly shallower than the adjacent waters. The plume of what appears to be high pigment concentrations may be caused by a combination of enhanced nutrients (due to the river outflow), dissolved organic matter, and higher nonorganic particle concentrations.

Although the CZCS sensor mission ended in 1986, near-real-time estimates of pigments and K values are routinely produced using NASA's current ocean color sensors known as SeaWiFS (Sea-viewing Wide Field of View Sensor)[6,7] and MODIS (Moderate Resolution Imaging Spectroradiometer).[8,9] Multiple passes

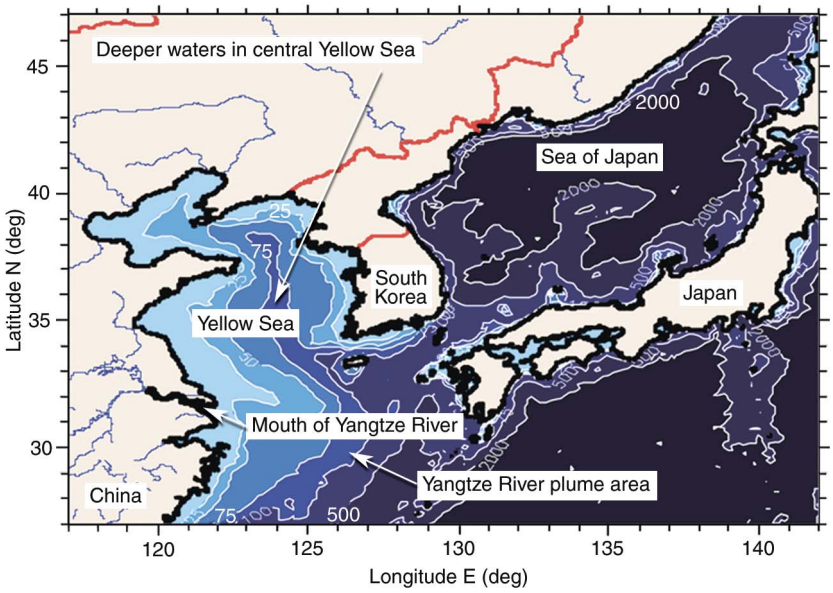

Figure 2. Yellow Sea and Sea of Japan bathymetry contours (in meters). The central Yellow Sea is deeper and clearer than the Yellow Sea coastal areas. In addition, the Yangtze River plume area is significantly shallower than the adjacent waters. The Sea of Japan, which generally has lower chlorophyll values than the Yellow Sea (see Fig. 1), is also much deeper than the Yellow Sea.

are often used to create a composite image that pastes together cloud-free pixels from consecutive passes. Although these images show impressive variability, they have no way of capturing the even more striking vertical variability that often exists. The remainder of this article focuses on the knowledge gained from *in situ* measurements that reveal the amazing degree of variability observed between the surface and the seafloor.

As an example, Fig. 3 shows beam attenuation coefficient profiles at 532 nm (c532) acquired in the Yellow Sea in July 2001. (The c532 data shown here and elsewhere are accurate to about 0.01/m.) The colors are chosen to illustrate the variability: blues and reds indicate a relatively minor increase of c532 with depth, and orange and green indicate a substantial increase with depth. In both cases the increase often is seen as an abrupt step-like change that occurs at various depths ranging from less than 20 to 55 m. There is a relatively clear surface layer atop a turbid nepheloid layer. The surface layer values can be <0.4/m, while the most turbid nepheloid values can exceed 8.0/m (i.e., a range of more than a factor of 20).

When the data are analyzed in terms of location (Fig. 4), at least three "subregions" are seen, each with its own distinct characteristics. Region A, the north-central (and deepest) parts of the Yellow Sea, has the weakest nepheloid layer c532 values, surface layers that are 20 to ≥30 m thick, and a bottom layer ≈30 m thick. Region B, closer to the Yangtze River plume, has the largest c532 values, surface layers that are ≈5 to 45 m thick, and a bottom layer ≈40 m thick. Region C (not shown) is an area of shallower waters to the west of Region A, and so it is not too surprising that nepheloid layers here tend to appear at a shallower depth than those in Region A. Region C has surface layers of about ≈0 to 40 m thick and a bottom layer about 25 m thick.

These same regions were surveyed in June 2001, and the c532 profiles showed essentially the same characteristics. Region A was also surveyed in October 2002, and those data were also quite similar to the data shown in Fig. 4. In other words, there is evidence of repeatability of the two-layer structure of a fairly clear surface layer and a relatively turbid (and thick) nepheloid layer.

The statistical relationship between the surface and nepheloid layer beam attenuation values is summarized in Fig. 5. In Regions A and C, the ratio between the nepheloid layer and surface layer is about a factor of 3.5 to 4.2, but in Region B it is between 10 and 11. Assuming that such "mean" relationships (within a given "region") can be shown to be reliable in other seasons or months, one has a way of extrapolating satellite-derived surface values down into the deeper layers.

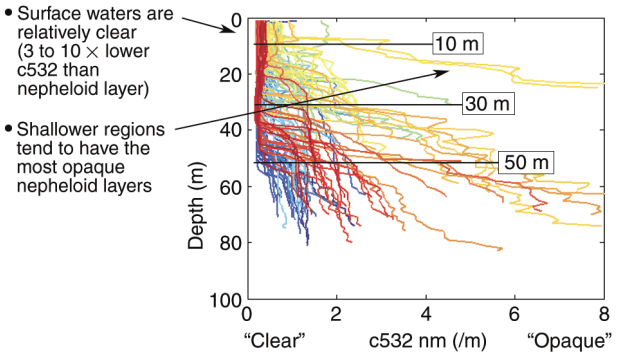

Figure 3. Summary of recurring optics features in the Yellow Sea. Blue and red indicate a relatively minor increase of c532 with depth; orange and green indicate a substantial increase with depth. In both cases the increase often is seen as an abrupt step-like change at various depths ranging from less than 20 to 55 m. There is a relatively clear surface layer atop a turbid nepheloid layer. All profiles exhibit an increase in turbidity (nepheloid layer) near the seafloor. The degree of optical variability increases with proximity to the seafloor, and optical clarity is *not* clearly related to the tide at locations >50 m deep.

To further quantify the nepheloid layer, we defined a threshold for being in the nepheloid layer (we set the threshold at c532 nm = 1.0/m) and then computed the thickness of the layer exceeding the threshold. We then created a color-coded map of the thicknesses, as shown in Fig. 6a. Here, the thickest nepheloid layers generally occur in Region B and the thinnest in Region A. Figure 6b shows a similar map for degree of opacity, computed as the mean c532 nm value in the bottom 10 m of each profile. Here, red indicates the most opaque (high c) values and green represents the clearest (low c) waters. (Red was chosen to indicate sites where optics-based sensors would have difficulty; green was chosen to indicate sites where those sensors would be more effective.)

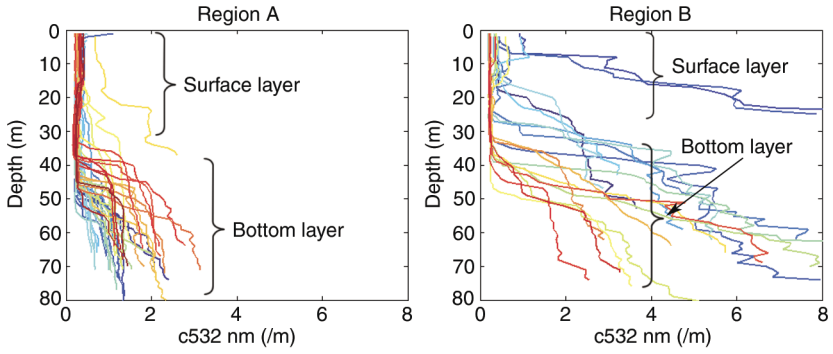

Figure 4. Optics spatial variability: c532 versus depth profiles in July 2001. Region A data from the north-central (and deepest) parts of the Yellow Sea have the weakest nepheloid layer c532 values, surface layers that are 20 to ≥30 m thick, and a bottom layer ≈30 m thick. Region B is closer to the Yangtze River plume and has the largest c532 values.

Besides investigating the patterns of spatial variability in optical clarity, we also attempted to determine the short-term (hours to days) temporal variability. Only one station was repeatedly sampled to provide this kind of information, i.e., the corner of Region C (near the boundary with Regions A and B; see Fig. 6a). The complete time series of c532 nm profiles is shown in Fig. 7a, and the data at three selected depths are shown in Fig. 7b. The shallow data exhibit almost no variability over the ≈48-h-long time series; those at 30- and especially 50-m depths show substantially more variability during this same time period. (Values reported for each depth were computed from an average at the given depth of ±2.5 m.) Data at the 50-m depth also have several "peaks" that are separated by about the expected semi-diurnal tidal period of 12 h.

If sediments were being stirred up during the periodic maxima in tidal flow, then one would expect a high positive correlation between currents and optical attenuation and scattering coefficients. To test this prediction we overlaid the ship's continuous record of current measurements, obtained with a range-gated Acoustic Doppler Current Profiler (ADCP), on top of the beam attenuation coefficient values. The magnitudes of the deepest available ADCP currents are shown in Fig. 8, along with the mean c532 nm value, computed between a 40- and 50-m depth in each profile. There is no obvious correlation between the optical data and the currents, suggesting that the sediments are too light to settle back to the seafloor during the lull between tidal maxima. (Note: the tidal currents are reversing direction between each of the maxima in Fig. 8, but since sediment resuspension does not depend on direction, we plotted the root-mean-square, or "rms," current amplitude.) It appears, therefore, that the relatively persistent nepheloid layers are the result of the continual stirring of these light

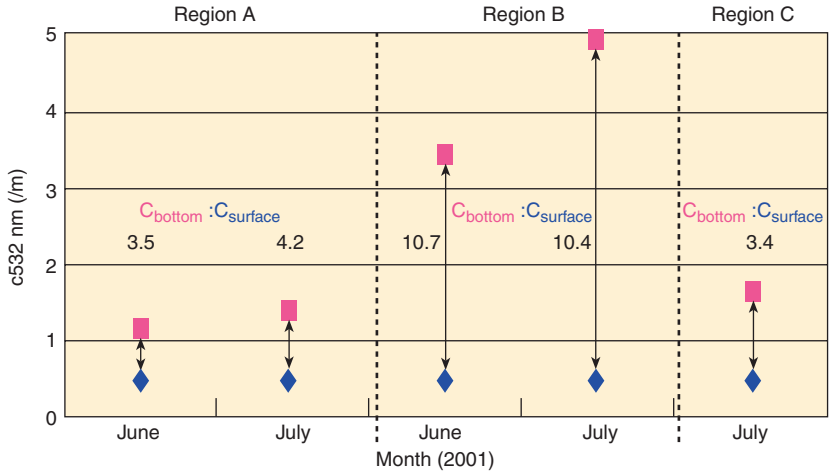

Figure 5. Relationship between Yellow Sea surface (diamonds) and bottom (rectangles) optics (mean beam c statistics). In Regions A and C, the ratio between the nepheloid layer and surface layer is about a factor of 3.5 to 4.2, but in Region B it is between 10.0 and 11.0.

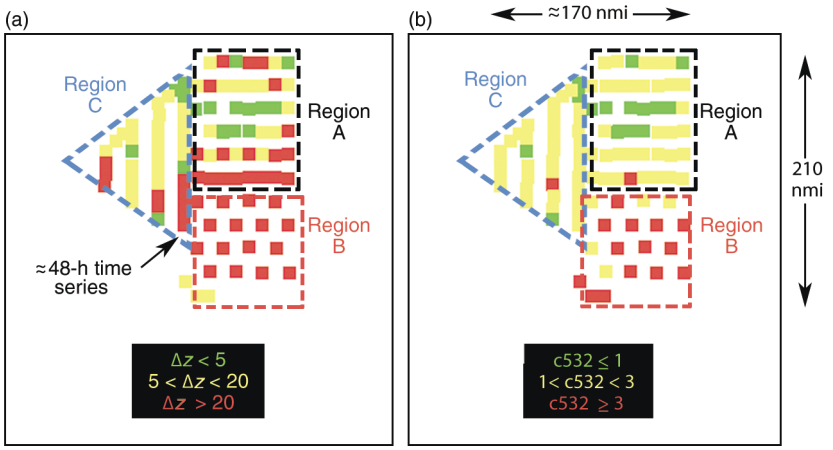

Figure 6. Nepheloid layer thickness and opacity in July 2001. (a) The thickest nepheloid layers (red) generally occur in Region B and the thinnest (green) generally occur in Region A. (b) Region B has the most opaque (high c) values (red), and Region A tends to have the clearest (low c) waters (green).

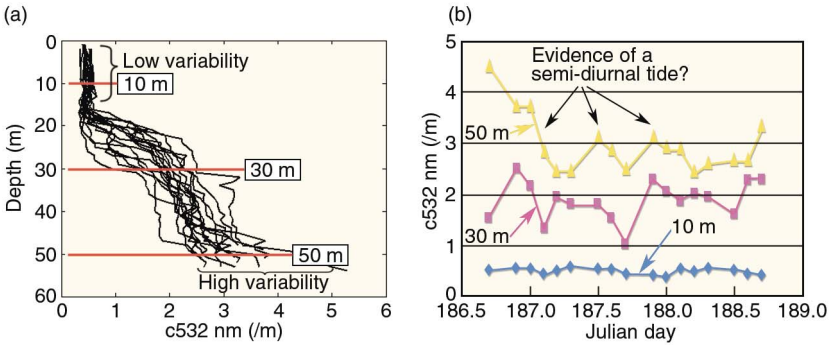

Figure 7. Temporal variability of beam attenuation. (a) Time series of c532 profiles at the corner of Region C (Fig. 6a). The shallow data exhibit almost no variability over the ≈48-h-long time series, while the data at 30- and especially 50-m depths show substantially more variability during this same time period. (b) Selected depths plotted versus date: The 30- and especially 50-m-deep c532 data have local maxima that are spaced at roughly the interval associated with a semi-diurnal tide.

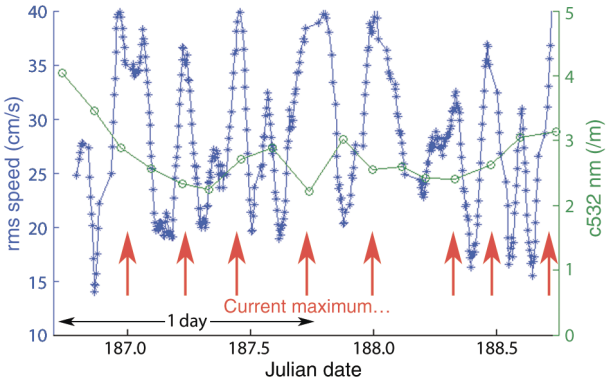

Figure 8. Temporal variability of bottom currents and optics. The comparison of magnitudes of the deepest available currents (blue) with near-bottom mean c532 nm values (green) shows no obvious correlation between the optical data and the currents, suggesting that the sediments are too light to settle back to the seafloor during the lull between tidal maxima. (Acoustic Doppler Current Profiler [ADCP] side lobes kept us from measuring all the way to the seafloor, so the deepest 10 m of each ADCP were used to compute these currents. The ADCP currents exhibited relatively little variability with depth.)

sediments by the relatively strong tidal currents and that the observed temporal variability in Fig. 7 is likely due to the advection of various concentrations of sediments at a given site.

The optical variability of the Yellow Sea can be summarized as follows:

- Near-surface waters (0–30 m) are relatively clear: K532 nm ≈ 0.1/m (same as off the coast of Panama City, Florida); c532 nm ≈ 0.4/m.
- All c and K profiles exhibit large increases at depth (due to sediments).
- Region B has the most salient nepheloid layers.
- Sediment effects on c and K tend to increase toward the west, and especially south of ≈34.5°N.
- The vertical extent of the nepheloid layer is predictable: ≈30 to 40 m above the seafloor.
- Beam attenuation is not clearly correlated with current speed, suggesting a sediment settling time constant much longer than the tidal cycle.

With regard to the last conclusion, a caveat should be made that these results are associated with data collected in waters that are generally at least 50 m deep. Dr. Sonja Gallegos (NRL-Stennis; personal communication) has made measurements in shallower regions within the Yellow Sea and reports a correlation between optical attenuation and tidal currents in such waters. More research is required that links tidal current speeds and sediment densities to the optical properties of the nepheloid layers.

Middle East Littoral

Several optical surveys have been conducted in the Persian Gulf, and they reveal optical characteristics that are similar to those observed in the Yellow Sea. Although we have not yet analyzed the Persian Gulf beam attenuation coefficient data, we have studied related optical properties: the optical backscattering coefficient b_b and the diffuse attenuation coefficient K. Of these, b_b is most sensitive to sediment concentrations, so it is used here to assess nepheloid layer characteristics.

Figure 9 shows the b_b profiles from two distinct (east and west) locations within the Persian Gulf. (The HOBILabs "a-Beta" sensor used to make these measurements has an accuracy of about 4 to 8%; for more details, see Ref. 10.) Unlike the optical profiles shown in Figs. 3, 4, and 7, these data have been plotted as a function of altitude off the seafloor. (This approach helps to emphasize the consistency of the nepheloid layers with respect to the source of sediments, and it also

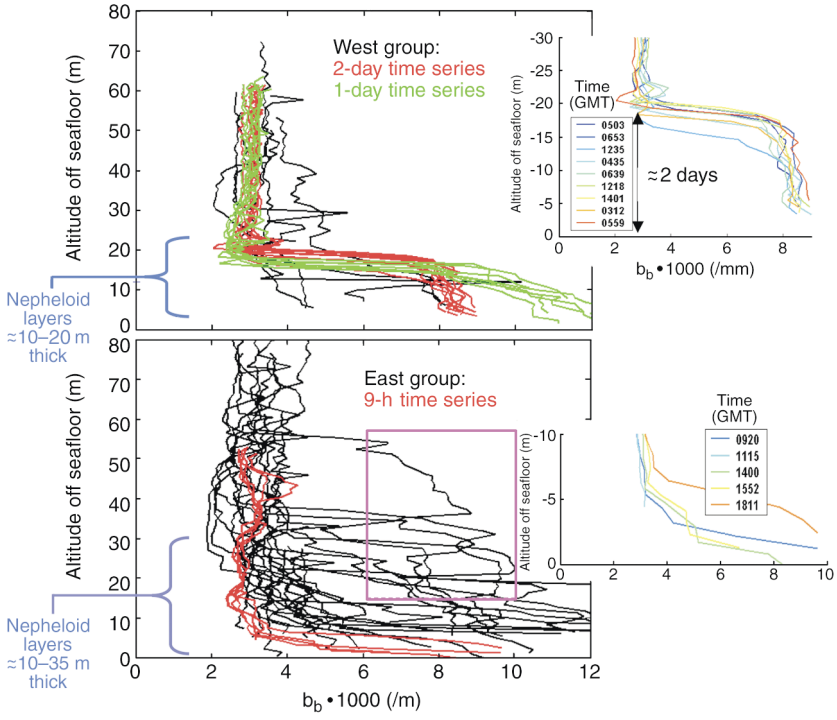

Figure 9. Persian Gulf optical backscattering (b_b) plotted versus height off the seafloor (Oct 2000). There are frequent occurrences of step-like transitions from low upper-layer scattering to high near-bottom scattering at about 10–35 m off the seafloor. Also, the east and west regions are clearly similar, even though their centers are separated by more than 250 nmi.

removes the possible confusion caused by varying water depths in the region.) Two features are worth noting in these data:

1. Frequent occurrences of step-like transitions from low upper-layer scattering to high near-bottom scattering at about 10–35 m off the seafloor
2. Similarity between the two regions even though their centers are separated by over 250 nmi

As indicated in Fig. 9, the Persian Gulf data include three different time series, all revealing the same major feature: although tidal currents in these areas are known to be up to 1 kt or more, the nepheloid layer b_b values remain relatively constant (and high) throughout periods that exceed a diurnal tidal cycle (i.e., about 12 h). This result suggests that the sediment settling time constant is much longer than the tidal cycle.

The east region also has data from three spatial series: two run approximately perpendicular to the bathymetry contours for the Persian Gulf and one runs roughly parallel to the bathymetry and is nearest to the Strait of Hormuz. The latter series includes the profiles enclosed within the magenta box in Fig. 9, i.e., the profiles having the unusually high b_b values at 20 to even 50 m off the seafloor. Considering that this location within the east region is likely to have the highest tidal currents, and that the currents will in turn stir up bottom sediments, it is not surprising that this location has some of the thickest and most opaque nepheloid layers.

The Persian Gulf October 2000 optical variability can be summarized as follows:

- Almost all b_b profiles have a maximum value in a nepheloid layer.
- The vertical extent of the nepheloid layer is predictable: about 10–20 m thick in the west and about 10–35 m thick in the east.
- West and east area nepheloid values are similar.
- Surface waters are relatively clear (K532 nm, not shown here, is about 0.10–0.15/m)

In addition, the time series results show that b_b has little temporal variability, suggesting a settling time constant for sediments that is much longer than the tidal cycle. Finally, the area near the Strait of Hormuz exhibits the thickest and most opaque nepheloid layers.

East China Sea

During the Littoral Warfare Advanced Development sea test (LWAD 03-4) in October 2003, optical measurements were made on the continental shelf of the East China Sea (Fig. 10). All of the data come from water depths between 100 and 200 m. The Kuroshio Current, which can exceed speeds of 2 kt, is mostly confined to a deep trough to the south and east of the LWAD 03-4 test site, but it occasionally encroaches onto the edge of the shelf area.[11] As a result of the scouring effect of this strong current system, one can predict little sediment to remain in the southeast corner of the test site, whereas more sediments are likely to occur in the northwest corner of the box (where depths are only about 100 m and currents are weaker). As shown in Fig. 11, the data support the following predictions: the thickest and most opaque nepheloid layers are farthest from the edge of the continental shelf (and from the Kuroshio Current), and the thinnest, least opaque nepheloid layers occur closest to the edge of the continental shelf.

The color-coded maps of nepheloid layer thickness and opacity (Figs. 11b and 11c, respectively) were created by choosing a nepheloid layer c532 nm threshold of 0.2/m. By comparison, the Yellow Sea threshold was 1.0/m (i.e., 5 times higher). Also, the maximum c532 values in the Yellow Sea exceed 8.0/m (see Fig. 3), compared to only about 1.3/m in the East China Sea. The lower East China Sea c532 values indicate a significantly lower overall sediment content than that seen in the Yellow Sea.

CONCLUSIONS

Our analysis of Yellow Sea, Persian Gulf, and East China Sea optics can be summarized as follows:

- Nepheloid layers are salient, persistent, and ubiquitous and are thicker and more opaque in the Yellow Sea than in the East China Sea. In addition, thickness may be predictable, varies for specific subregions in the three geographic areas studied, and does not

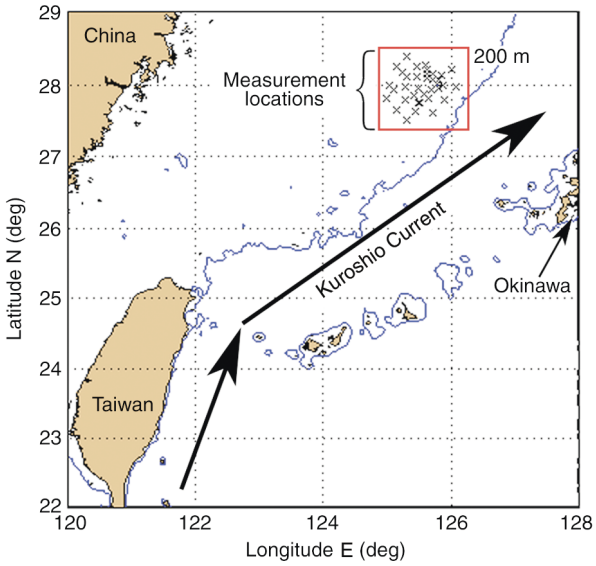

Figure 10. East China Sea optical measurement locations. Measurements were made on the continental shelf of the East China Sea in water depths between 100 and 200 m. The Kuroshio Current, which can exceed speeds of 2 kt, is mostly confined to a deep trough to the south and east of the measurement locations but occasionally encroaches onto the edge of the shelf area. As a result of the scouring effect of this strong current system, little sediment is expected to remain in the southeast corner of the test site, whereas more sediment is likely to occur in the northwest corner of the box.

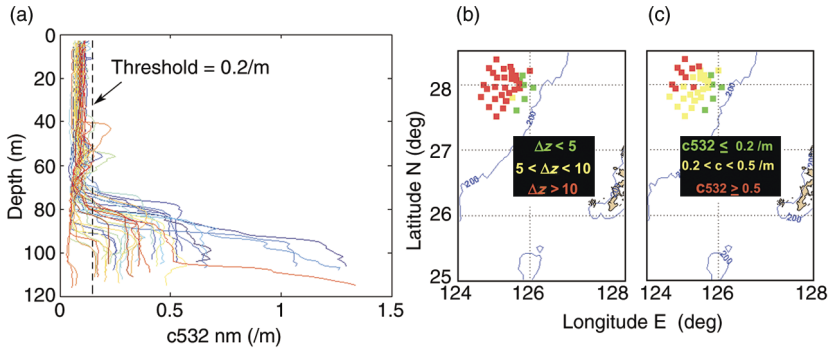

Figure 11. Nepheloid layer characteristics in the East China Sea. (a) Beam attenuation profiles: As in the Persian Gulf and Yellow Sea, surface layers are relatively clear but there is a step-like change upon entering the nepheloid layer. Note that the Yellow Sea threshold for defining the nepheloid layer was 5 times higher than the value of 0.2/m selected here. (Colors do not denote nepheloid thickness in this plot.) (b) Nepheloid layer thickness: The thickest nepheloid layers (red) are farthest from the edge of the continental shelf (and from the Kuroshio Current), and the thinnest (green) occur closest to the edge of the continental shelf. (c) Nepheloid layer opacity: The most opaque nepheloid layers (red) are farthest from the edge of the continental shelf, and the least opaque (green) occur closest to the edge of the continental shelf. Panels (b) and (c) also show the 200-m-depth contour obtained from the NAVOCEANO Digital Bathymetric Database (DBDB-V).

appear to vary with tidal cycle. (Caveat: All these results apply to waters that are generally at least 50 m deep; tidal currents are more likely to affect nepheloid layers in shallower waters.)

- Surface waters are much clearer than bottom waters (c_{bottom}:c_{surf} can exceed 10), and the ratio between bottom and surface waters may be predictable (c_{bottom}:c_{surf} variations in the Yellow Sea ranged from 3.4 to 10.7, depending on location).

Based on these observations, we recommend developing computer-aided tools for mine countermeasures (MCM) commanders and ASW planners that incorporate this knowledge of surface optics and nepheloid layers. Specifically, the tools should allow users to specify a system's optical wavelength and its maximum range in optical attenuation lengths. (Alternatively, system-specific tactical decision aids could be built that incorporate these parameters.) The tools should provide depth-integrated optical attenuation from the surface downward and from the bottom upward. These depth-integrated parameters are computed as follows:

$$\text{Attenuation lengths} = \int_0^z c(z')\,dz' ,$$

where z can refer to either the depth below the surface or the altitude off the seafloor. The tools should also allow users to specify a required surface penetration range or a desired altitude off the seafloor for system operation.

The relatively low c532 values observed in the surface waters of the central Yellow Sea, Persian Gulf, and East China Sea indicate that an airborne system like ALMDS or LASH should work well in these areas. However, near-bottom systems like AN/AQS-20X and AQS-24 may have difficulties seeing through nepheloid layers. To better quantify these difficulties, sensor-specific analysis is needed that includes the computation of the number of optical attenuation lengths for a designated system deployed at a specific height above the seafloor (e.g., at around 9 m).

In determining the environmental optics impact on the penetration range of airborne sensors, one can use a combination of historical, nowcast (remote sensing), and forecast (modeling) data. The focus of this article has been on describing the historical knowledge acquired through various *in situ* measurement surveys. In the future, one could also rely on autonomous undersea vehicles (AUVs) such as the glider AUVs recently developed at Webb Research Corporation (WRC).[12] By equipping these AUVs with optical sensors, updated optical profile data could be obtained just before the start of a military conflict, or even after the commencement of hostilities. Another possible source for updated *in situ* data is from the MCM (or ASW) system itself (for example, a lidar-based system provides estimates of the optical properties of the ocean[13]). It is therefore important to incorporate any system-sensed performance into the MCM and ASW evaluation tools.

One also needs to account for conflicting requirements on a hybrid MCM system. For example, a bottom mine-hunting system that uses acoustics to detect a mine-like object and optics to identify it could easily have conflicting altitude constraints. In particular, the AN/AQS-20/24 systems use side-scan sonar detectors and optical identification sensors. Analysis is required to identify the impact of nepheloid layers on the AN/AQS-20/24 to see if the altitude for effective side-scan operations is incompatible with optical system performance for contact reacquisition and identification. More analysis is also needed to identify the impact of expected/measured bottom optical properties on divers and neutralization AUVs for reacquire/identify/neutralize missions.

A primary concern for the Navy should be whether persistent nepheloid layers preclude the use of optical systems in some near-bottom environments. As an alternative to optical systems, the Navy should consider the wisdom of continuing to develop high-frequency imaging sonars such as the Dual Frequency Identification Sonar (DIDSON).[14]

For regions where optical sensors are being deployed, the Navy needs to incorporate sensing strategies that

include the collection of full water column *in situ* optical profiles to support mission planning. As mentioned above, one particularly useful tool is the glider AUV equipped with optical sensors. Prototype expendable sensors have also been developed that could be launched from air, surface, or subsurface platforms.

In conclusion, recent measurements of littoral optical properties have been made that provide valuable insight into the potential impact of ambient optical conditions on various optics-based naval systems. The analysis of these data has shown that significant spatial variability exists that could be used to help predict the utility of those systems. The knowledge gleaned from these data could also be used to develop tactical decision aids that would help MCM and ASW commanders to plan future missions.

REFERENCES

[1]Hojerslev, N. K., "A History of Early Optical Oceanographic Instrument Design in Scandinavia," in *Ocean Optics*, R. W. Spinrad et al. (eds.), Oxford University Press, Inc., pp. 118–147 (1994).

[2]Apel, J. R., "Jerlov Water Types," in *Principles of Ocean Physics*, Academic Press, pp. 580–585 (1990).

[3]Smart, J. H., "Seasonal and Spatial Variations in the Absorption of Light in the North Atlantic Ocean," *Johns Hopkins APL Tech. Dig.* **14**(3), 231–243 (1993).

[4]Ruda & Associates, Inc., *Hypersepctral Imaging*, http://www.ruda.com/Hyperspectral.htm.

[5]Morel, A., "Optical Modeling of the Upper Ocean in Relation to Its Biogenous Matter Content (Case I Waters)," *J. Geophys. Res.* **93**(C9), 10,749–10,768 (Sep 1988).

[6]SeaWifS Web site, http://seawifs.gsfc.nasa.gov/SEAWIFS.html.

[7]Hooker, S. B., and McClain, C. R., "The Calibration and Validation of SeaWiFS Data," *Prog. Oceanogr.* **45**(3-4), 427–465 (2000).

[8]MODIS Web site, http://modis.gsfc.nasa.gov/.

[9]Gregg, W. W., and Woodward, R. H., "Improvements in Coverage Frequency of Ocean Color: Combining Data from SeaWiFS and MODIS," *IEEE TGARS* **36**(4), 1350–1353 (Jul 1998).

[10]Maffione, R. A., and Dana, D. R., "Instruments and Methods for Measuring the Backward-Scattering Coefficient of Ocean Waters," *Appl. Optics* **36**(24), 6057–6067 (Aug 1997).

[11]Kaneko, A., Gohda, N., Koterayama, W., Nakamura, M., Mizuno, S., and Furukawa, H., "Towed ADCP Fish with Depth and Roll Controllable Wings and Its Application to the Kuroshio Observation," *J. Phys. Oceanogr.* **49**, 383–395 (1993).

[12]Webb Research Corporation Web site, *SLOCUM Glider*, http://www.webbresearch.com/slocum.htm.

[13]Smart, J. H., and Kwon, K. H., "Comparisons Between *in situ* and Remote Sensing Estimates of Diffuse Attenuation Profiles," in *Laser Remote Sensing of Natural Waters: From Theory to Practice*, V. I. Feigels and Y. I. Kopilevich (eds.), *Proc. SPIE* **2964**, pp. 100–109 (Nov 1996).

[14]DIDSON Web site, http://www.apl.washington.edu/programs/DIDSON/DIDSON.html.

ACKNOWLEDGMENTS: This work was supported in part by the Office of Naval Research (ONR) Grant # N000149810773; the World-wide Ocean Optics Database (WOOD) is funded by Dr. Steve Ackleson (Code 322OP).

THE AUTHOR

JEFFREY H. SMART has spent more than 26 years in the field of ocean environmental studies since joining APL in 1978. He received his M.S. in atomic physics in 1977 from Wayne State University and a B.S. in physics in 1975 from Oakland University. He is the Laboratory's leading expert on ocean optics and optics-related environmental characterizations using historical databases and satellite data and is nationally known for his work. Mr. Smart is the Project Manager for the ONR-funded World-wide Ocean Optics Database (http://wood.jhuapl.edu). He is a member of the American Geophysical Union and the Alliance for Remote Sensing. His e-mail address is jeff.smart@jhuapl.edu.